Larsen, H.C., Duncan, R.A., Allan, J.F., Brooks, K. (Eds.), 1999
Proceedings of the Ocean Drilling Program, Scientific Results, Vol. 163

7. COMPOSITION OF VOLCANIC ROCKS FROM THE SOUTHEAST GREENLAND MARGIN, LEG 163: MAJOR AND TRACE ELEMENT GEOCHEMISTRY[1]

Lotte Melchior Larsen,[2] J. Godfrey Fitton,[3] and Andrew D. Saunders[4]

ABSTRACT

During Leg 163, in the Southeast Greenland margin, drilling penetrated a thick succession of volcanic rocks that erupted during breakup of the North Atlantic in the early Tertiary. Samples recovered during Leg 163 supplement the samples recovered during Leg 152 from the transect across the volcanic margin at 63°N. During Leg 163, drilling at Site 989 was intended to recover the oldest part of the continental prebreakup series, and drilling at Site 990 was intended to penetrate the transition zone from synbreakup, compositionally variable volcanic products, to postbreakup volcanics with a limited compositional range and a depleted chemical character similar to mid-ocean-ridge basalts (oceanic character). All the lava flows recovered from Sites 989 and 990, however, have an oceanic chemical character with low contents of incompatible elements and high contents of Sc. A dikelet from Site 990 and a previously drilled dike from Site 917 are likewise oceanic. We consider that the two drilled lava flows from Site 989 were emplaced after breakup despite their setting on the innermost part of the continental margin.

The succession at Site 990 consists of 13 units of lava flow that show a slight compositional development upsection with Mg# decreasing from ~62 to ~49. This variation is within the limits known from the slightly younger oceanic succession drilled earlier at Site 918, in which the variation is thought to reflect fractionation in magma chambers in the oceanic crust. The reestablishment of magma chambers after the breakup must have been achieved during the interval that the short, undrilled lava succession between uppermost Site 917 and lowermost Site 990 was deposited.

All the lava flows from Sites 989 and 990, except perhaps one (Unit 989-1), are crustally contaminated, as judged from their high Ba/Zr (>0.42) ratios. The two dikes appear to be uncontaminated. The contamination most likely took place in magma chambers in the young oceanic rift, which, at this early stage of spreading, could still have contained fragments of continental crust. Most lavas were probably erupted within the rift and flowed subaerially away from it toward the edge of the continent. The dikes show that lateral injection of magma into the continental crust also took place without resulting in crustal contamination. The oceanic lava flows at Site 989 on the innermost margin have probably been erupted through such laterally injected dikes.

The primary magma for the postbreakup rocks is estimated to have contained ~18% MgO. After fractionation of 30 mol% olivine ($Fo_{91–82}$), it shifted to gabbro fractionation, and the magmas started to erupt. The modal composition of the gabbroic cumulate is 8% olivine ($Fo_{82–74}$), 50% plagioclase ($An_{76–66}$), and 42% clinopyroxene ($Fs_{9–15}$). The erupted oceanic magmas are produced by <24 mol% gabbro fractionation, with an average of 14%. Thus, geochemical modeling indicates that the oceanic crust is composed of olivine cumulates (30%), gabbro cumulates (14%), and melts (lava flows and dikes, 56%), which is in accordance with models based on geophysical data.

INTRODUCTION

The Southeast Greenland rifted continental margin (Fig. 1) possesses a thick succession of seaward-dipping lava flows, known from seismic sections as seaward-dipping reflector sequences (SDRS). These volcanics were erupted during breakup of the North Atlantic in the early Tertiary (e.g., Larsen and Saunders, 1998; also reviewed by Saunders et al., 1997). The objective of Leg 163 at the Southeast Greenland margin was to complete a transect across the margin at 63°N, which had been initiated during Leg 152, and to obtain rock samples for a parallel transect at 66°N (Duncan, Larsen, Allan, et al., 1996). The drilled cores from Legs 152 and 163 cover a large part of the volcanic stratigraphy, in particular the earlier part of the succession with the important transition from prebreakup continental volcanism to postbreakup oceanic volcanism (Larsen, Saunders, Clift, et al., 1994; Fitton et al., 1995, 1998a, 1998b).

During Leg 163, some of the earliest oceanic volcanic rocks immediately overlying the breakup transition zone were drilled at Site 990. A hole intended to cover the earliest part of the continental succession was also drilled (Site 989). This paper presents the major and trace element composition of the rocks from the 63°N transect recovered during Leg 163 and places them within the combined succession obtained from Legs 152 and 163. Complementary trace element and isotope data for a subset of samples are presented and discussed by Saunders et al. (Chap. 8, this volume). Also during Leg 163, we drilled a hole on the planned 66°N transect but recovered only one fresh lava flow. Data for this flow are included in Saunders et al. (Chap. 8, this volume) and are not addressed in this paper.

SUMMARY OF EARLIER RESULTS FROM THE 63°N TRANSECT

Figure 2 shows the 63°N transect across the Southeast Greenland margin. Site 917, drilled during Leg 152, comprises three volcanic series. The lower series consists of tholeiitic basalts to picrites at various stages of fractionation, whereas the middle series consists of more fractionated rocks: siliceous basalts, tholeiitic andesites, and dacites. The magmas that gave rise to both these lava series are inter-

[1]Larsen, H.C., Duncan, R.A., Allan, J.F., Brooks, K. (Eds.), 1999. *Proc. ODP, Sci. Results*, 163: College Station, TX (Ocean Drilling Program).

[2]Geological Survey of Denmark and Greenland, Thoravej 8, DK-2400 Copenhagen NV, Denmark. Also: Danish Lithosphere Centre, Oster Voldgade 10, DK-1350 Copenhagen K, Denmark. lml@geus.dk

[3]Department of Geology and Geophysics, Grant Institute, University of Edinburgh, West Mains Road, Edinburgh EH9 3JW, United Kingdom.

[4]Department of Geology, University of Leicester, Leicester LE1 7RH, United Kingdom.

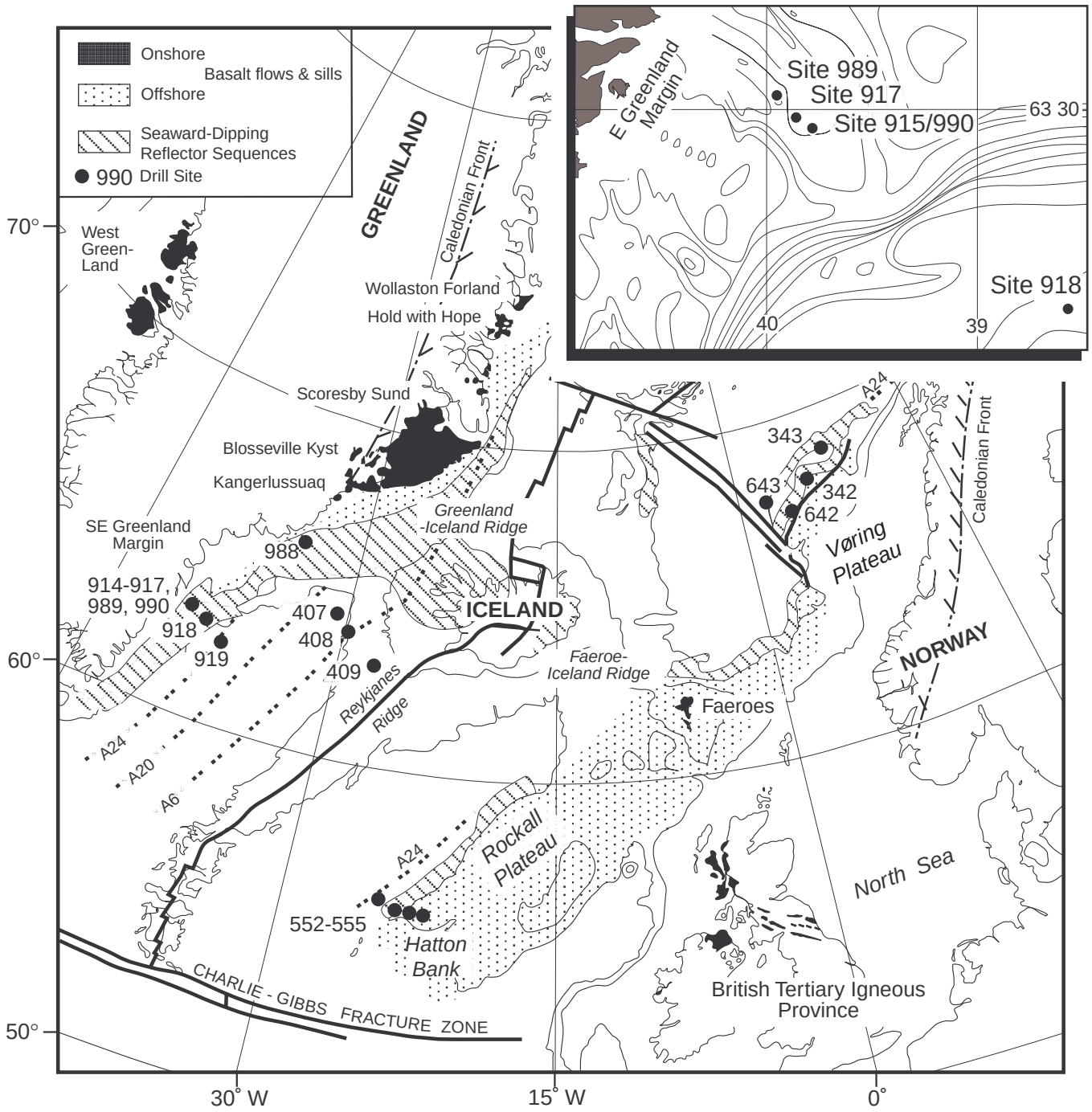

Figure 1. Map of the North Atlantic region showing the main physiographic features and some of the earlier ODP drill sites. Modified after Larsen, Saunders, Clift, et al. (1994). Inset shows details of the drill sites along the 63°N transect across the Southeast Greenland margin.

preted as having fractionated in magma chambers in the continental crust (Larsen, Saunders, Clift, et al., 1994; Fitton et al., 1995, 1998a, 1998b). The chemical and isotopic composition of these magmas, notably their high Ba and Sr contents and low $^{143}Nd/^{144}Nd$ and sometimes high $^{87}Sr/^{86}Sr$ isotopic values, suggest that they have been contaminated first by continental crust in granulite facies and later by continental crust in amphibolite facies (Fitton et al., 1998a). The most evolved rocks are also the most contaminated, as expected for fractionation and assimilation in crustal magma chambers.

The upper series at Site 917 is separated from the middle series by a fluvial sandstone that may represent a significant time interval (from ~60 Ma to ~57 Ma) (Sinton and Duncan, 1998; Tegner and Duncan, Chap. 6 this volume). The upper series consists of olivine basalts and picrites showing variable degrees of fractionation, inter-

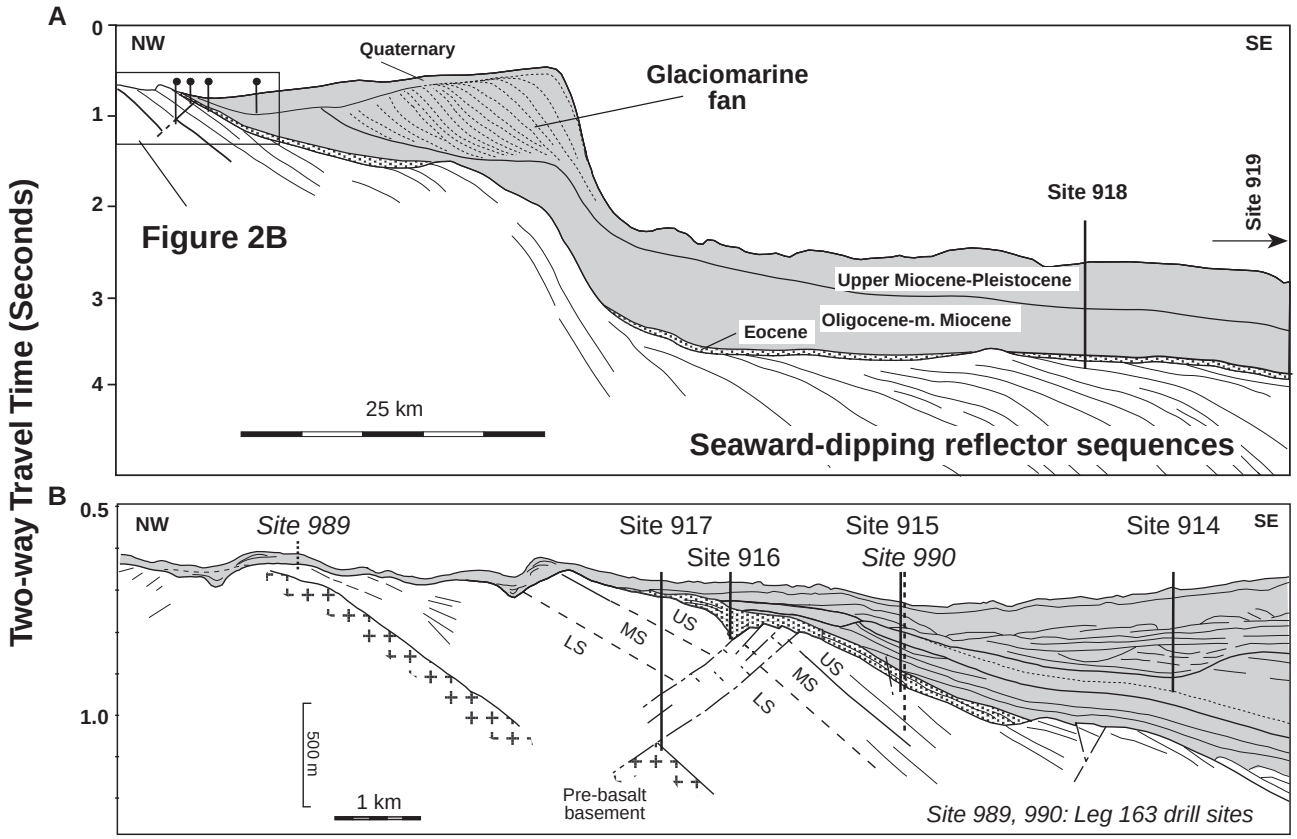

Figure 2. **A.** Section across the Southeast Greenland margin at 63°N. **B.** Locations of the sites drilled during Legs 152 and 163 and discussed in this paper. Modified after Larsen, Saunders, Clift, et al. (1994).

preted as erupted during final continental rupture when magma chambers were transient or nonexistent, allowing access of primitive Mg-rich magma to the surface (Fitton et al., 1995, 1998b). Some of the upper series lavas still show evidence of slight crustal contamination (Fitton et al., 1998a).

Sites 915 and 918, situated 70 km apart in the postbreakup part of the SDRS, contain basaltic lavas with a restricted compositional range. These lavas are interpreted as having been filtered through magma chambers in the crust at the spreading oceanic ridge (Larsen, Saunders, Clift, et al., 1994; Fitton et al., 1995, 1998a, 1998b); however, the single lava flow recovered from Site 915 shows slight contamination by continental crust (Fitton et al., 1998a). The overall similarity between the basalts at the two sites suggests that, after continental breakup, the composition of the lavas forming the SDRS was relatively constant.

Sites 915 and 917 are situated only 3 km apart, and the stratigraphic distance between the drilled successions is considered to be no more than a few hundred meters (Fig. 2). Yet this interval between the drilled successions must contain the transition from the variable synbreakup volcanics at Site 917 to the compositionally limited postbreakup volcanics. Site 990, drilled during Leg 163, was designed to penetrate this transition zone (Duncan, Larsen, Allan, et al., 1996).

At the continental end of the 63°N transect, the character of the most landward and possibly oldest lavas in the SDRS wedge, as well as the nature of the basal unconformity and the underlying basement, was not determined from the Leg 152 work. Site 989 was aimed at penetrating both volcanics and basement, with the expectation that the volcanic succession recovered would either be a lateral equivalent of the Site 917 lower series or older (Duncan, Larsen, Allan, et al., 1996).

In the following, the prebreakup volcanics composing the Site 917 lower and middle series are designated the continental succession; the synbreakup volcanics in the Site 917 upper series form a transition zone, and the postbreakup volcanics comprising Sites 915, 990, and 918 are designated the oceanic succession, even though some of the oceanic rocks, as will be discussed, are contaminated with continental crustal material. For reasons discussed below, the Site 989 volcanics are included in the oceanic series.

ANALYTICAL METHODS

The samples were ground in an agate Tema swing mill at the University of Edinburgh, and splits of identical powders were used for all the different analyses noted below.

Major elements were analyzed at the Geological Survey of Denmark and Greenland, Copenhagen. Most elements were determined by X-ray fluorescence (XRF) analysis on fused glass discs. The rock powders were dried at 110°C for 2 hr and ignited at 1000°C for 1 hr with subsequent determination of the loss on ignition (LOI). The ignited samples were mixed with sodium tetraborate in the ratio 0.7500 g sample to 5.2500 g borate and fused in Pt/Au crucibles under continuous agitation for 1–1½ hr. After inspection for homogeneity, the melts were poured into Pt/Au molds creating glass discs with 32 mm

Table 1. Major and trace element analyses of basalts from Leg 163.

Hole:	989A	989B	989B	989B	989B	989B	990A	990A	990A	990A	990A	990A	990A	990A	990A	990A	990A
Core, section	2R-3	5R-2	10R-2	10R-7	11R-1	13R-2	1R-1	1R-1	1R-1	1R-2	1R-2	3R-1	3R-1	5R-4	7R-3	8R-4	9R-3
Interval (cm):	68-81	41-47	9-15	59-64	58-64	120-126	71-75	90-98	137-141	27-31	56-62	10-18	60-66	79-85	34-39	26-32	76-82
Piece:	3	3A	2	5A	7	16	11	14	20	6	11	2	7	3	1A	3A	3C
Depth (mbsf):	12.12	22.60	65.92	73.32	74.68	81.30	182.71	182.90	183.37	183.77	184.06	191.70	192.20	216.89	224.64	235.68	244.33
Unit:	989-1	989-1	989-1	989-1	989-2	989-2	990-clast	990-clast	990-clast	990-clast	990-clast	990-clast	990-clast	990-1	990-1	990-2	990-2
Major elements (wt%):																	
SiO_2	50.22	50.18	49.91	49.99	50.43	50.62	45.66	43.09	49.28	48.17	50.13	50.59	49.62	51.16	51.09	50.61	50.88
TiO_2	1.064	1.084	1.006	1.033	0.914	0.901	1.225	1.214	1.387	2.501	1.593	1.591	1.118	1.256	1.198	0.959	0.964
Al_2O_3	13.68	13.61	13.71	13.41	14.17	14.17	17.70	17.98	19.94	18.58	20.60	20.88	14.73	13.80	13.57	15.16	15.33
Fe_2O_3	4.84	4.73	5.39	6.11	2.64	2.31	4.16	5.29	5.55	5.58	4.47	5.14	4.18	4.95	3.90	4.66	2.89
FeO	8.03	8.38	7.29	7.01	8.71	8.95	4.50	6.26	4.44	4.62	4.06	3.37	7.65	8.44	9.69	6.90	8.06
MnO	0.22	0.23	0.20	0.20	0.21	0.20	0.29	0.27	0.08	0.16	0.10	0.11	0.18	0.20	0.23	0.21	0.19
MgO	7.27	7.14	7.94	8.03	7.87	7.65	5.23	6.05	4.51	4.30	3.74	3.33	7.57	6.21	6.44	6.99	6.83
CaO	11.60	11.49	11.20	10.67	12.39	12.50	11.58	8.41	8.22	9.05	7.36	7.69	11.14	10.35	10.33	11.26	11.58
Na_2O	2.25	2.16	2.05	2.11	1.95	1.88	2.51	2.38	3.41	3.16	3.63	3.90	2.46	2.46	2.21	2.12	2.16
K_2O	0.078	0.064	0.057	0.117	0.099	0.056	1.349	1.374	0.839	1.067	1.382	1.323	0.142	0.268	0.224	0.226	0.194
P_2O_5	0.116	0.109	0.089	0.095	0.090	0.087	0.203	0.175	0.244	0.405	0.310	0.353	0.102	0.126	0.123	0.109	0.098
Volatiles:	1.13	1.18	1.34	1.33	0.77	0.81	4.91	6.76	1.95	2.11	1.97	1.63	1.16	0.92	1.15	1.14	0.94
Sum:	100.50	100.35	100.18	100.10	100.24	100.13	99.32	99.26	99.86	99.71	99.33	99.89	100.04	100.13	100.14	100.35	100.09
Mg#:	54.28	53.35	56.97	56.50	58.94	58.37	56.19	52.63	49.15	47.45	48.32	45.70	57.30	49.32	49.65	56.03	56.45
Trace elements (ppm):																	
Nb	2.4	2.7	1.9	2.1	2.2	2.0	1.7	1.8	1.9	19.2	2.5	2.6	2.0	3.5	3.4	2.4	2.1
Zr	62	58	45	52	47	46	67	65	80	118	94	87	57	72	67	56	57
Y	30	28	24	25	24	23	49	53	22	38	29	26	28	33	33	25	25
Sr	74	71	69	68	84	83	185	162	512	488	555	715	82	98	93	113	119
Rb	1.1	0.6	0.9	1.6	1.7	1.3	5.5	8.4	5.1	13.1	7.5	7.1	1.8	2.3	2.0	1.9	1.6
Th	0.0	1.0	0.7	0.4	0.6	0.6	0.6	0.0	0.0	1.6	0.4	0.9	0.9	0.3	0.9	0.9	0.3
Pb	0.0	1.6	0.3	0.0	0.2	25.5	102.1	1.1	3.5	1.7	3.5	3.5	0.5	0.9	1.2	1.2	1.8
La	4	1	5	2	2	4	8	8	11	21	14	12	2	4	4	4	5
Ce	8	9	7	7	10	7	24	23	29	45	35	37	6	15	11	13	12
Nd	8	9	4	7	7	6	21	20	19	36	26	25	7	10	8	8	7
Zn	98	102	88	91	85	86	104	79	85	128	80	108	101	104	106	88	85
Cu	195	211	195	190	151	151	177	192	115	115	126	107	135	190	102	69	115
Ni	73	69	80	75	96	103	322	280	71	72	79	56	99	54	51	70	72
Co		61	56	64	51	50	52	43	27	29	31	26	81	53	49	44	46
Cr	50	49	54	54	219	229	1825	1845	42	148	64	53	110	36	36	128	129
V	383	413	409	390	328	327	378	400	312	408	363	354	395	394	371	314	309
Ba	15	19	19	17	34	21	107	89	452	405	512	613	28	59	60	58	69
Sc	48	53	52	54	51	52	57	67	49	50	55	48	62	55	51	50	46
Ga		16	16	17	16	15	19	18	22	23	26	24	18	18	17	17	16

diameter. The XRF spectrometer used was a Phillips PW1606 multichannel instrument with a Rh-anode X-ray tube. Calibration and correction for background and line overlaps were calculated from measurements on synthetic single-element glass discs, and corrections for matrix effects were calculated either from measurements on synthetic glass discs or from the absorption coefficients of Heinrich (1966).

Na_2O was determined by atomic absorption spectrometry (AAS). Each dried sample (0.25–0.5 g) was treated with hydrofluoric acid in a PTFE beaker on a hotplate. After evaporation to dryness, the residue was dissolved in a 50 ml hydrochloric acid/potassium chloride solution and sodium measured on a Perkin Elmer PE2280 AAS instrument.

For FeO determination, each dried sample (0.1 g) was treated with ammonium vanadate/hydrofluoric acid overnight. Boric acid and a measured amount of iron(II) was added. Surplus iron(II) was determined by automatic potentiometric titration using Cr(VII) as titrant. The method used is a modification of that used by Wilson (1955).

Volatiles were calculated as the weight LOI corrected for the calculated gain of weight created by the oxidation of iron(II) to iron(III) during ignition.

As shown by L.M. Larsen et al. (1998b), the accordance between the major element analyses carried out in Copenhagen and Edinburgh is excellent, ensuring full compatibility between the present major element data set and that for the Leg 152 samples obtained in Edinburgh (Fitton et al., 1998b).

Trace elements were analyzed by XRF on pressed powder pellets at University of Edinburgh, in the same laboratory and with the same methods as described by Fitton et al. (1998b) for the Leg 152 samples.

A subset of samples was also analyzed at the University of Leicester by instrumental neutron activation analysis and at the NERC Isotope Geoscience Laboratory for Sr, Nd, and Pb isotopes; these results are presented by Saunders et al. (Chap. 8 this volume).

RESULTS

The analytical results are presented in Table 1. Mg# is calculated as 100 $Mg/(Mg + Fe^{2+})$ (atomic%), with the iron oxidation adjusted to $Fe_2O_3/FeO = 0.15$ (wt%).

All the analyzed basalts are altered to some extent. Glass and olivine are altered to smectitic and saponitic clays, and vesicles are lined or filled with clay and carbonate (Teagle and Alt, Chap. 13, this volume). Elements known to be mobile during such alteration are primarily K, Rb, and Ba, and variations in these elements should be treated with caution. Also, major elements, such as Na, Mg, and Si,

Table 1 (continued).

Hole:	990A	990A	990A	990A	990A	990A	990A	990A	990A	990A	990A	990A	990A	990A	990A	990A	917A
Core, section	13R-3	15R-2	15R-5	16R-3	17R-3	18R-6	19R-5	21R-1	21R-4	22R-1	22R-3	22R-6	23R-2	23R-4	24R-1	24R-3	26R-2
Interval (cm):	97-103	68-74	8-14	111-115	109-115	76-82	64-70	86-92	77-82	47-53	24-30	68-73	41-47	132-138	15-18	16-20	83-89
Piece:	9A	2B	1	5	2C	3A	9	2E	4B	4	2A	1D	2B	10B	3	2A	13
Depth (mbsf):	263.93	271.49	275.05	278.82	282.97	296.10	305.16	309.06	313.38	318.37	321.06	325.63	329.17	332.96	337.25	340.03	213.10
Unit:	990-3A	990-3A	990-3B	990-4	990-5	990-6	990-7	990-8	990-9	990-10	990-11	990-11	990-11	990-12	990-dike	990-13	917-39 (dike)
Major elements (wt%):																	
SiO_2	49.40	50.63	50.19	50.77	50.68	50.33	50.36	50.16	50.93	50.23	50.88	50.36	50.98	50.21	49.57	50.58	49.89
TiO_2	0.938	0.942	0.982	0.980	0.959	0.968	0.939	0.738	0.877	0.751	0.859	0.859	0.777	0.755	1.757	0.799	0.816
Al_2O_3	15.02	14.96	15.15	14.67	14.60	14.29	14.32	16.45	15.03	16.00	14.18	15.83	15.99	16.26	14.64	14.04	13.83
Fe_2O_3	6.21	2.36	4.87	3.79	3.33	2.89	3.08	3.61	3.67	4.41	4.78	3.35	5.25	3.92	4.91	4.39	5.95
FeO	5.84	8.54	6.86	7.37	7.98	7.71	7.77	5.92	6.21	5.70	6.56	6.59	4.80	5.96	7.02	6.76	5.91
MnO	0.21	0.20	0.22	0.19	0.22	0.22	0.21	0.18	0.20	0.17	0.20	0.22	0.17	0.19	0.20	0.19	0.17
MgO	7.19	7.05	6.78	7.07	7.18	8.02	8.09	7.09	7.78	7.14	7.57	7.47	6.67	7.13	6.02	7.84	7.31
CaO	11.65	11.73	11.60	11.42	11.78	12.10	11.68	11.62	11.62	11.22	10.27	12.02	11.52	11.62	10.84	11.13	11.82
Na_2O	2.15	2.09	2.15	2.13	2.20	1.98	2.03	1.95	2.15	1.93	1.94	2.14	2.09	1.96	2.36	1.86	2.05
K_2O	0.193	0.140	0.301	0.140	0.081	0.114	0.111	0.141	0.110	0.159	0.212	0.088	0.222	0.113	0.286	0.253	0.495
P_2O_5	0.091	0.092	0.092	0.103	0.100	0.101	0.083	0.073	0.086	0.078	0.083	0.090	0.092	0.076	0.161	0.064	0.036
Volatiles:	1.18	0.94	1.05	1.32	0.91	1.13	1.20	1.90	1.51	2.10	2.43	1.13	1.56	1.91	1.52	2.15	1.44
Sum:	100.06	99.68	100.26	99.95	100.01	99.85	99.87	99.84	100.18	99.90	99.95	100.15	100.13	100.11	99.29	100.07	99.71
Mg#:	55.98	57.21	54.95	56.99	56.94	61.15	60.82	61.00	62.32	59.88	58.49	61.12	58.63	60.32	51.55	59.71	56.78
Trace elements (ppm):																	
Nb	2.0	2.0	2.1	2.2	2.4	2.7	2.1	1.7	2.0	1.7	1.6	2.1	1.4	1.5	3.1	1.2	1.2
Zr	53	52	53	56	56	49	49	40	47	41	44	46	42	40	102	39	39
Y	26	25	27	26	25	23	25	18	22	18	22	22	21	20	37	20	25
Sr	90	90	87	107	113	107	73	104	94	88	81	98	96	91	112	71	70
Rb	2.6	1.5	3.4	1.5	0.4	1.0	0.7	1.2	0.4	2.7	3.2	1.1	1.8	1.9	2.6	4.3	29.0
Th	1.2	0.6	0.5	0.0	0.2	0.6	0.2	0.3	0.9	0.5	0.5	0.3	0.5	0.5	1.1	0.6	0.9
Pb	0.7	3.1	0.8	1.1	19.1	1.1	1.1	0.6	0.8	0.2	0.0	1.0	0.6	1.0	0.7	0.0	1.1
La	3	2	4	4	5	5	4	1	3	4	3	3	2	3	4	0	2
Ce	9	11	11	14	13	8	8	7	10	9	8	12	10	9	13	8	9
Nd	7	7	6	10	10	7	6	6	9	6	5	7	6	6	12	4	6
Zn	87	86	93	89	88	83	89	64	72	68	78	73	71	70	121	84	86
Cu	91	119	75	131	140	107	167	79	100	57	82	141	78	54	252	56	69
Ni	77	74	84	87	84	96	97	93	125	108	113	98	83	103	72	104	73
Co	48	47	53	50	48	48	50	40	51	44	49	46	43	44	47	50	60
Cr	132	132	136	156	158	212	214	239	250	249	216	230	229	241	98	247	128
V	332	320	358	323	334	322	343	251	302	253	266	295	257	255	471	301	314
Ba	34	32	37	52	50	57	26	276	37	26	27	37	80	24	10	18	13
Sc	49	50	54	50	49	52	57	41	51	41	41	48	43	42	65	51	52
Ga	16	17	17	17	18	16	17	16	15	16	15	16	17	16	20	15	16

may be mobile, but we have not found any evidence of significant loss or gain of these elements in the Leg 163 samples. There is also no evidence in the Leg 163 samples for mobility of yttrium, as found in the basalts from Site 918 (L.M. Larsen et al., 1998b).

Site 989

Site 989 is located 43 km from the Southeast Greenland coast. Hole 989B penetrated to 84.2 meters below seafloor (mbsf). The underlying basement was not reached. In total, 80 m of basalt were drilled, which form only two flow units. Unit 989-1 (see Table 1 to correlate units with standard Ocean Drilling Program core designations) is at least 69 m thick and is the thickest lava flow yet recorded from a SDRS (Duncan, Larsen, Allan, et al., 1996). It is a compound flow of aphyric basalt consisting of a number of flow lobes, 0.1–10 m thick, and the three analyses from this unit show some slight intraflow variability, with MgO = 7.1%–8.0%. Unit 989-2 is a massive flow of sparsely phyric basalt at least 11 m thick, and the two analyses from this unit are very similar. Moreover, there are only slight compositional differences between Unit 989-1 and 989-2, the largest being lower FeO* and higher CaO and Cr in Unit 989-2.

The basalts at Site 989 are evolved, with Mg# = 53.4–58.9 and MgO = 7.22%–8.16% (calculated free of volatiles). They have low TiO_2, K_2O, Rb, Sr, Nb, Zr, and rare earth element (REE) contents. As already shown on board ship, they are distinctly different from the basalts at Site 917, especially from the Site 917 lower series basalts with which they were originally thought to correlate (Duncan, Larsen, Allan, et al., 1996) but which have much higher Ba and Sr than the Site 989 basalts. The Site 989 basalts show much greater similarities to the postbreakup successions at Site 990 and Site 918, as discussed below.

Site 990

Site 990 is located 52 km from the Southeast Greenland coast, very close to the previously drilled Site 915, which it was intended to extend. The volcanic succession at Site 990 is overlain by two sedimentary units of probable Eocene age (Duncan, Larsen, Allan, et al., 1996). Unit I is an ~10-m-thick mixed cobble conglomerate from which almost only cobbles without matrix were recovered. These consist of highly altered basalt, gabbro, dolerite, quartzite, and siltstone. The depositional environment indicated is active erosion in a high-relief area and is interpreted as a high-gradient stream or a fan delta (Duncan, Larsen, Allan, et al., 1996). The underlying Unit II is an ~20-m-thick, dark brown, clayey volcaniclastic breccia with highly altered angular clasts, interpreted as a debris flow originating from the

altered top of the volcanic pile (Duncan, Larsen, Allan, et al., 1996). Beneath Unit II is the reddened and completely altered top of the uppermost lava flow.

The volcanic succession was drilled from 211.9 mbsf to the bottom of the hole at 342.7 mbsf. This 130.8-m interval contains 13 lava flows, most of them with red-oxidized flow tops. In addition, Unit 990–12 contains a small chilled vein or dikelet of basalt, which will be considered as a separate unit. The lithology of the basalts varies from aphyric to plagioclase-olivine phyric, with additional minor augite phenocrysts in some flows.

Cobble Conglomerate Clasts

Seven of the mafic clasts in the conglomerate were analyzed to determine the provenance of the eroded material, specifically to search for indications that the Site 917 lower series was exposed and being eroded, because this succession is 450 m thick at Site 917 but appears to be completely missing at Site 989, only 5 km farther west. The lowermost clast is large (22 cm cored), and chemically it is in all respects identical to the underlying lava succession at Site 990, despite the ~20-m-thick debris flow between the cobble conglomerate and the lava pile. The overlying six smaller clasts have a consistently different chemical character. They are high-Al, high-K basalts with low Fe and high Ba and Sr. Their trace elements and ratios are rather variable. A shipboard analysis of a similar clast was interpreted by Duncan, Larsen, Allan, et al. (1996) as derived from the lower series at Site 917 because of the high Ba and Sr. However, the consistent chemical character of the six clasts analyzed (Table 1) makes this interpretation unlikely. Only three of the 28 analyzed lower series basalts have such high K_2O contents, and none of them has the high Al_2O_3 and low total FeO of the clasts (Fitton et al., 1998b; L.M. Larsen et al., 1998a). We believe that the clasts are derived from an altogether different mafic association, possibly belonging to the Precambrian basement. It is not surprising that elevated basement on the continental margin should be available for erosion during breakup.

Thus, there are no positive indications that the Site 917 lower series was being eroded. The reason why the series is missing at Site 989 may rather be depositional offlap of the volcanic pile toward the embryonic rift zone, although erosion or faulting cannot be excluded.

Volcanic Succession

The basalt lava flows at Site 990 are evolved, with Mg# = 49.3–62.3, MgO = 6.27%–8.23%, and low contents of incompatible elements. They are generally quite similar to the basalts from Site 989 and the single basalt from Site 915. An exception is the dikelet in Unit 990–12 that, at a similar degree of fractionation, is considerably more enriched in incompatible elements than any of the lava flows.

The drilled lava succession shows only limited compositional variation, for example, TiO_2 = 0.7%–1.3%. Some trace elements

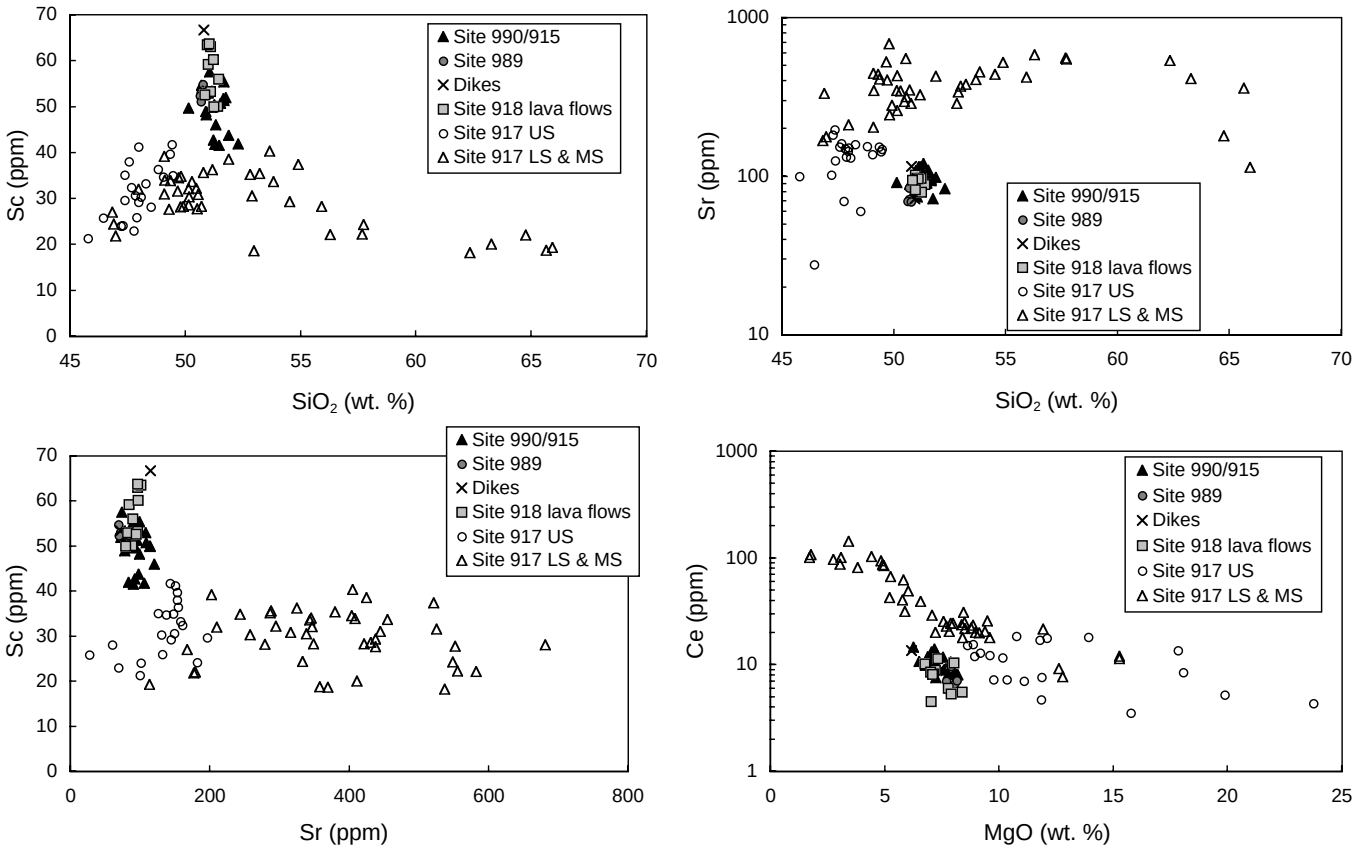

Figure 3. Variation diagrams illustrating the chemical differences between the pre- and synbreakup succession (open symbols: Site 917 lower, middle, and upper series) on one hand, and the postbreakup oceanic rocks drilled at Sites 915, 918, and 990 (solid symbols) on the other hand. In each plot, the oceanic rocks form a tight, well-defined cluster set apart from the earlier rocks because of their high Sc and relatively low Sr and Ce. The lava flows from Site 989 and the two dikes from Site 917 and 990 clearly have oceanic chemistry. One dike symbol is always hidden by other symbols in the cluster.

show larger variations, e.g., Cr = 250–36 ppm, Zr = 39–72 ppm, and Ba = 24–276 ppm. As discussed below, the variation can be explained by crystal fractionation of the magmas.

DISCUSSION

Oceanic vs. Continental Magma Compositions

We have earlier (Fitton et al., 1995, 1998b; L.M. Larsen et al., 1998a; Saunders et al., 1998) demonstrated the differences in chemical composition between the relatively uniform postbreakup oceanic basalts at Sites 915 and 918 and the much more variable compositions in the pre- and synbreakup volcanics at Site 917. All the lava flows recovered at Site 989 and 990 have chemical compositions similar to the oceanic basalts at Site 915 and 918. This is illustrated by the four variation diagrams in Figure 3. In all four plots, the basalts from Sites 915, 918, 989, and 990 lie together in a single, well-defined tight cluster, which is completely separated from both the continental and the synbreakup volcanics at Site 917. The basalts at Site 989 and 990 are of indisputable oceanic character, with higher Sc and lower Ce (and other light REEs) than the continental and synbreakup volcanics. They also have lower MgO and higher SiO_2 than the synbreakup volcanics.

The volcanics from the 63°N transect include two dikes, one in the Site 917 middle series (Unit 917–39; L.M. Larsen et al., 1998a, included here in Table 1) and one that cuts Unit 990-12. Both of these dikes have an oceanic chemical character, and in Figure 3 they plot within the tight cluster of basalts from Sites 915, 918, 989, and 990.

Figure 4 shows TiO_2 vs. Mg# for the basalts of Sites 989, 990, 915, 918, and the two dikes. The synbreakup series (Site 917 upper series) is shown for comparison. The basalts plot in a number of parallel trends that can be explained as fractionation trends, as detailed later. Site 917 upper series comprises two parallel trends, interpreted as belonging to magmas formed by different degrees of partial melting, smaller degrees of melting producing higher contents of TiO_2 in both primary and derivative melts (L.M. Larsen et al., 1998a; Fitton et al., 1998b; Fram et al., 1998). The most evolved basalts from the synbreakup series show similar degrees of fractionation to the least evolved basalts from Site 990 (Mg# = 60–63). All the postbreakup lavas and the dike from Site 917 plot within one, or perhaps two, trends with some of the basalts from Site 918 having the highest TiO_2. The dikelet in Unit 990–12, with its higher contents of incompatible elements, seems to have arisen from a separate magma batch produced by smaller degrees of melting or from a different source (Saunders et al., Chap. 8, this volume).

Development with Time

Figure 5 shows the upsection development in Mg# in a combined section through the syn- and postbreakup succession at Sites 917 and 990/915. A gap is inserted between the two to show the undrilled interval. The single lava flow from Site 915 occupies a stratigraphic position immediately above Site 990.

The other oceanic rocks are also shown in Figure 5, placed on top of the 917–990/915 succession in accordance with their younger age. Site 918 is clearly the youngest, being situated 70 km farther offshore from Site 990, and the stratigraphical gap between these two sites is considerable. Ar/Ar dating of the two flows from Site 989 (Tegner and Duncan, Chap. 6, this volume) has shown that they have the same age as those from Site 990 (~56 Ma), thus confirming that the flows at Site 989 belong to the postbreakup stage despite their position in the innermost part of the SDRS. The upper flow at Site 989 shows normal magnetic polarity, whereas the lower flow shows reversed magnetic polarity. The two uppermost flows at Site 990 also show normal magnetic polarity, whereas the other flows at Site 990 and the

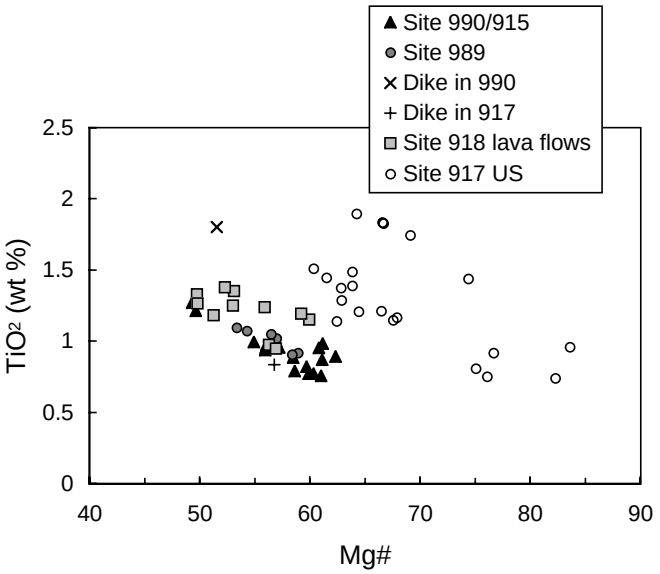

Figure 4. TiO_2 vs. Mg# for the oceanic rocks, with the synbreakup rocks from Site 917 upper series shown for comparison. Individual trends of increasing TiO_2 with decreasing Mg# can be explained as resulting from crystal fractionation within individual magma batches.

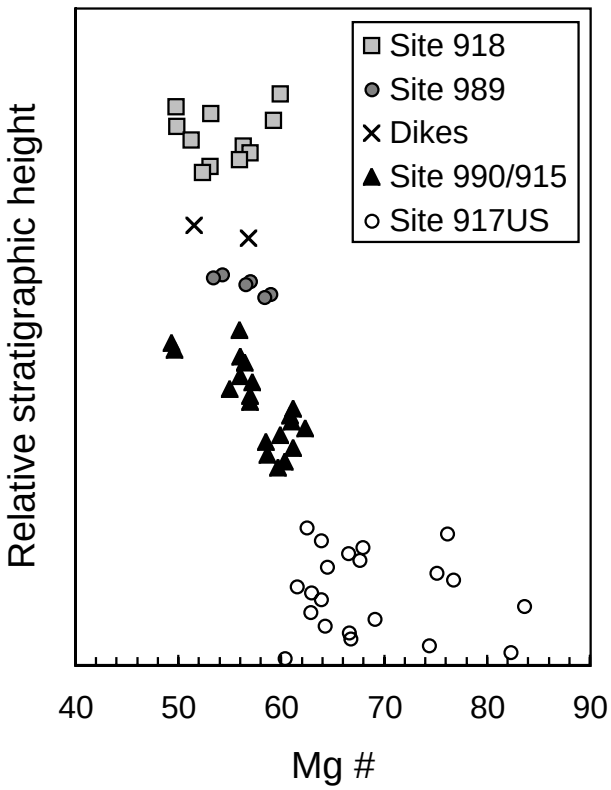

Figure 5. Development in Mg# in a combined section through the syn- and postbreakup basalts. The lava successions are placed on top of each other in accordance with their inferred relative age. It is possible that the lava flows from Site 989 are exactly coeval with the uppermost flows from Site 990, as detailed in the text. The two dikes are, for comparison, placed in the void between Sites 990 and 918.

one at Site 915 show reversed magnetic polarity (Duncan, Larsen, Allan, et al., 1996). The normal magnetic polarity interval represented is probably C25n (Tegner and Duncan, Chap. 6, this volume). It is thus possible that the flows at Site 989 are exactly coeval with the upper flows at Site 990, but, for the sake of comparison, they have been placed above Site 990/915 in Figure 5.

The minimum ages of the two dikes are unconstrained, and for comparison they have been placed in Figure 5 in the "void" between Sites 989 and 918.

Figure 5 shows that there is a slight but distinct decrease in Mg# upsection through the flows at Site 990, from Mg# = 60–62 to Mg# = ~50. The Shipboard Scientific Party noticed that Zr increases and Cr and Ni decrease with height upsection, indicating increasing degrees of evolution (Duncan, Larsen, Allan, et al., 1996). Site 990 appears to consist of three flow groups: Units 13 to 6, with Mg# = 62.3–58, Zr = 39–49 ppm, Cr = 250–212 ppm, Ni = 125–83 ppm; Units 5 to 2, with Mg# = 58–55, Zr = 52–57 ppm, Cr = 158–128 ppm, Ni = 87–70 ppm; and Unit 1 with Mg# = ~49, Zr = 67–72 ppm, Cr = 36 ppm, Ni = 52–54 ppm. The flow from Site 915 is similar to Units 990-5 to 990-2. Site 915 is situated only 150 m northeast of Site 990, and it is difficult to imagine that Units 990-1 and 990-2 (both normally magnetized), with a combined thickness of ~90 m, should not be present at Site 915 below the drilled flow. Unit 990-1 is probably an unusually differentiated flow. It also has a very low Cr/Ni ratio of 0.7, an unusual (but not exceptional) value for a North Atlantic Tertiary basalt. Unit 989-1 likewise has Cr/Ni = 0.7, despite higher Mg# (and MgO) than Unit 990–1, which corroborates the possibility that these two flows could be coeval and even related. Unit 989-2 is most similar to Units 990-13 to 990-6.

The flows at Site 918 cover close to the same range in major and trace element compositions as those at Site 990 and, despite the signs of systematic development upsection at Site 990, we must conclude that the conditions that only allowed magmas within a fairly narrow compositional range to be erupted had been established before the flows at Site 990 were deposited. As in earlier works (Larsen, Saunders, Clift, et al., 1994; Fitton et al., 1995, 1989b), we believe this filtering happens in magma chambers in the new-formed oceanic crust. Thus, the allegedly short, undrilled interval between the Site 917 upper series and Site 990 must comprise the transition from syn- to postbreakup conditions. There is little indication of whether the transition is abrupt or gradational. Fram et al. (1998) suggest an increase in the degree of melting with time, but most of this increase takes place between the Site 917 upper series and Site 915. Data such as the Zr/Sc relations shown in Figure 6 suggest completely separate magmatic systems. Perhaps lavas from the two magmatic systems form interfingering flows over a short interval, as seen in the Faeroe Islands upper series (Gariépy et al., 1983; Waagstein, 1988).

Figure 6 is a plot of Zr vs. Sc for the syn- and postbreakup basalts. This was used by Fitton et al. (1998b) to demonstrate that the much higher Sc in the oceanic rocks can be an effect of thinning of the lithospheric lid with time, thus allowing more of the melting to take place in spinel-facies mantle, where Sc is relatively incompatible during melting. The new data for the oceanic basalts from Site 989 and 990 fall on exactly the same trend as Site 915 and 918; the less evolved lowermost units 990-13 to 990-6 just extend the trend to less fractionated compositions. Thus, after breakup no further gradual shallowing of the melting column is indicated.

The same conclusion can be reached from considerations of the major element compositions. SiO_2 is sensitive to pressure during melting (McKenzie and Bickle, 1988; Niu and Batiza, 1991; Kinzler and Grove, 1992, 1993), and the high and similar SiO_2 contents (≥50% irrespective of slight contamination; see below) in the oceanic rocks from all sites indicate final melt segregation at low pressures corresponding to conditions beneath an oceanic ridge, right from the beginning of the postbreakup stage. Synbreakup basalts at a similar

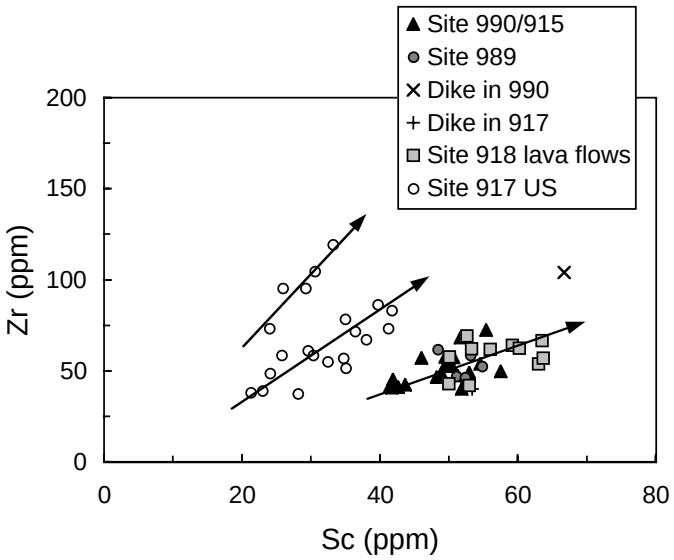

Figure 6. Zr vs. Sc for the syn- and postbreakup basalts. The arrows show three discrete fractionation trends. Except for the dike from Site 990, all the postbreakup oceanic basalts follow the same trend, indicating that the melting conditions for the primary magmas stayed constant after breakup and that no further shallowing of the average melting depth took place. See text for details.

Table 2. Fractionation of calculated primitive magma, Site 990.

Major elements	Primitive magma	Fractionated from primitive	Unit 990-7	Fractionated from primitive	Unit 990-1
SiO_2	48.45	51.17	51.19	51.69	51.83
TiO_2	0.71	0.95	0.95	1.32	1.27
Al_2O_3	10.89	14.60	14.56	13.88	13.98
FeO total	11.21	11.02	10.72	14.05	13.07
MnO	0.16		0.21		0.20
MgO	18.01	7.92	8.23	6.23	6.29
CaO	8.88	11.91	11.87	10.00	10.48
Na_2O	1.54	2.07	2.06	2.35	2.49
K_2O	0.08	0.11	0.11	0.16	0.27
P_2O_5	0.06	0.08	0.08	0.12	0.13
Sum:	99.99	99.82	100.00	99.80	100.00
Crystallized (%):		30		54	
Assemblage:		ol		ol + pl + cpx	
Pressure (kbar):	7	7-3		3	
Temperature (°C):	1449	1202		1171	

Notes: Primitive magma calculated by adding equilibrium olivine to Unit 990-7 until MgO = 18%. Fractionation calculations done with the program COMAGMAT at FMQ oxygen buffer and pressure as indicated. The fractionated from primitive column is the last step of olivine fractionation. At 31 mol% crystallized the fractionating assemblage is ol + pl + cpx. See text for detailed explanation.

stage of differentiation (Mg# = 63–60) have lower SiO_2 contents, average 48.9%, compared to an average of 51.2% in the oceanic rocks (calculated free of volatiles). Even though the Site 990 basalts are slightly contaminated (see below), the difference is in the order of 2% SiO_2, corresponding to a relative shallowing of the average melting pressure in the order of 3–5 kbar during the final breakup (Niu and Batiza, 1991; Kinzler and Grove, 1993).

Based on trace elements, Fram et al. (1998, fig. 6) modeled the oceanic basalts (Sites 915 and 918) as generated at 25–17 kbar by 10%–12% melting. The models of Niu and Batiza (1991), Kinzler and Grove (1992, 1993), and Langmuir et al. (1992) for calculating the conditions of generation (for polybaric incremental melting) of oceanic basalts of known major-element composition can also be ap-

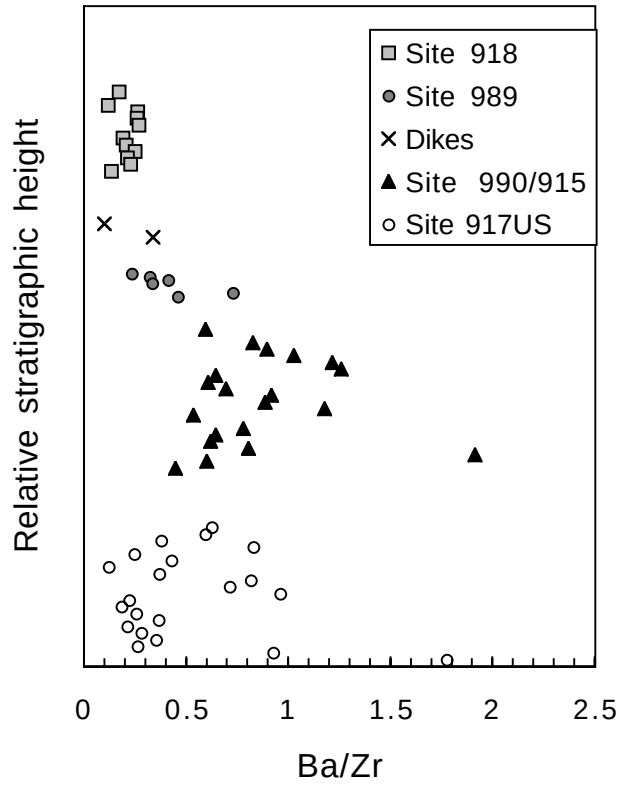

Figure 7. Variation of Ba/Zr in the same composite section through the syn- and postbreakup basalts used in Figure 5. All the lava flows from Site 990 and one from Site 989 have elevated Ba/Zr and are interpreted as contaminated with continental crustal material. One lava flow from Site 989 and the two dikes appear to be uncontaminated.

plied to the fractionated magma composition from Site 990 with ~8.0% MgO (Table 2, column 2). Although the results vary between the models, all three models indicate that melting started at high pressures (33–20 kbar) and high temperatures (1580°–1460°C), resulting in high degrees of melting (15–21 wt%). The results for Site 990 are very similar to the results for a basalt from the Reykjanes Ridge calculated by Kinzler and Grove (1993), but higher pressures and degrees of melting are indicated than for the trace-element–based model of Fram et al. (1998).

Crustal Contamination

Figure 7 shows the variation in Ba/Zr within the same composite succession as in Figure 5. Increased Ba/Zr has been used as an indicator of crustal contamination (Larsen, Saunders, Clift, et al., 1994; Fitton et al., 1998a, 1998b; L.M. Larsen et al., 1998a). Figure 7 shows that, while the Site 918 basalts consistently have a Ba/Zr of <0.3, many Site 917 upper series basalts and almost all Site 989 and 990 basalts have a Ba/Zr of >0.3, although not as high as the Ba/Zr values of 2–5 (up to 22) found in the continental series. Could this slight elevation in Ba/Zr be caused by crustal contamination of the syn- and earliest postbreakup basalts? Saunders et al. (Chap. 8, this volume) present REE and isotope data showing that this is indeed the case. Most of the Site 989 and 990 basalts for which there are REEs and isotope data have elevated light REEs, low Pb isotope ratios, low Nd and high Sr isotope ratios. There is a very good correlation between high Ba/Zr and low $^{206}Pb/^{204}Pb$, indicating that the elevated Ba/Zr is not caused by secondary introduction of Ba during alteration. Only one isotopically analyzed lava flow, Unit 989-1, and the dikelet in Unit 990–12 appear to have uncontaminated isotopes, and these are also among the few rocks with low Ba/Zr (<0.42). If Ba/Zr >0.42 is used as an indicator of contamination, then Figure 7 shows that all of the lava flows at Site 990 and also Unit 989-2 are crustally contaminated, as are several of the Site 917 upper series basalts. Both dikes appear to be uncontaminated. As shown by Fitton et al. (1998a), contamination by subcrustal lithospheric mantle is a possibility that cannot be excluded, but it is not required to explain the data.

Based on trace elements and isotope ratios, Saunders et al. (this volume) model a contamination process where the primary magma is bulk contaminated with 2%–5% gneiss, followed by ~30% olivine fractionation. Most trace elements are explained by addition of up to 2% gneiss. The gneiss sample used has 63.6% SiO_2, and incorporation of 2% of such material should give rise to an increase in SiO_2 of about 0.3% before and 0.4% after fractionation. An increase in SiO_2 of this size is on the limit of what is detectable in a natural data set. Unit 989–1 and the two dikes do have SiO_2 contents which are lower than in most of the other rocks, but in total there is no significant difference between the SiO_2 contents of the contaminated oceanic basalts and the uncontaminated ones from Site 918 (Fig. 3). The major elements thus suggest a maximum of 2% bulk gneiss contamination in accordance with the conclusions from the trace elements. The 5% contamination indicated by the Pb isotopes is probably a result of selective contamination with crustal Pb because of the great contrast in the contents of Pb in the two rock types.

Oceanic Basalts on the Continental Margin

As related in the summary of earlier results, the magmas of the continental series are considered to be fractionated and contaminated in magma chambers in the continental crust; the synbreakup series is variable and Mg-rich because magma chambers at breakup were transient or nonexistent; and the limited compositional range of the erupted oceanic rocks was acquired when magma chambers became re-established, this time in oceanic crust. However, despite their oceanic-type chemistry, all the flows at Site 989 and 990 are crustally contaminated except one (Unit 989–1, ironically one of the two flows resting on relatively thick continent in the inner part of the continental edge; Fig. 2). If the magmas were contaminated in the magma chambers, then these chambers must sit in, or be in contact with, continental crust. Alternatively, the magmas may have been contaminated when passing through the continental crust on their way to the surface.

Based on a deep seismic profile, regional gravity data, and an Iceland-type crustal accretion model for the postbreakup volcanic rocks, H.C. Larsen et al. (1998) estimated that the thinned wedge of the continent that constitutes the continent-to-ocean transition zone is ~45 km wide on the 63°N transect and that Site 917 is situated on thinned continent 25 km from the outer edge (Fig. 8). The syn- and postbreakup volcanics were envisaged to have accumulated, fractionated, and extruded within the new oceanic rift zone at the outer edge of the continent. The rift zone was envisaged as standing above sea level so that the lavas flowed subaerially inland to their present positions of ~25 km from the rift. If this were so, then the magmas could not have become crustally contaminated. On the other hand, the young oceanic rift zone, just after breakup, must have been situated immediately adjacent to the continental edge. There are three possible ways in which the early oceanic magmas could have come in contact with continental crustal material.

1. The magma accumulation zone would still have extended beneath the continental wedge. Magma that failed to be focused into the rift zone could have been trapped in magma chambers within the wedge and been extruded up through it, thus by-

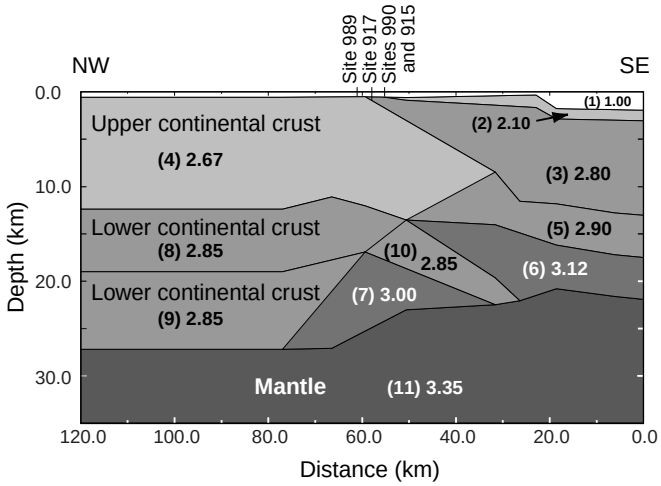

Figure 8. Crustal structure of the Southeast Greenland margin at 63°N, as modeled from reflection seismic and regional gravity data by H.C. Larsen et al. (1998). The model shown is the one preferred by H.C. Larsen et al. (1998) of two possible models; more recent wide-angle seismic data have confirmed that it is the best one (T. Dahl-Jensen, pers. comm., 1997). Numbers in parentheses are the original numbers of the crustal segments defined by H.C. Larsen et al. (1998), and the succeeding numbers are the densities used to fit the modeled gravity to the measured gravity. Oceanic crustal segment number 3 consists of SDRS with known thicknesses of up to 7 km plus ~2 km of dikes. Crustal segments numbers 5 and 6 are cumulates, and the boundary between them is arbitrary. Crustal segment number 7 is interpreted as igneous underplated material, and segment number 10 as a semidetached sliver of the lower continental crust. The thickness of the layers of the oceanic crust modeled by the geophysical data shown, and modeled by the calculations based on geochemical data as described in the text, are compared in Table 3. See text for details.

passing the rift itself. This mechanism is expected to produce magmas more similar to those of the continental series than to those of the oceanic series. Magmas that bypass the center of a rift zone and are erupted on older crust are known from other areas including oceanic ridges, and they tend to be compositionally different from those being erupted at the rift axis. We do not believe that this mechanism gave rise to the contamination in the oceanic basalts.

2. The young oceanic rift zone could still have contained torn slivers and foundered blocks of continental material. This is a simple and straightforward explanation that fits the observations. The magmas could be contaminated or not, depending on the character of the sidewall in the local magma chambers. The slivers of continental material need not be so large as to show up on seismic profiles; however, the seismic profile given by H.C. Larsen et al. (1998) does show evidence that the continental edge was ragged and that a megasliver had formed (Fig. 8).
3. The magmas could have been emplaced laterally from the rift into the continent and extruded locally. The two dikes provide evidence that such a process did take place, in addition to the second possibility favored above. The dike from Site 917 sits in the strongly contaminated middle series, yet it is clearly oceanic in chemistry and is even uncontaminated. This strongly suggests lateral injection into the continent from the oceanic rift zone, and it also shows that this can take place without contamination of the magma. The dikelet in Unit 990-12 is clearly from another melt batch (Fig. 4) from a different mantle type (mid-ocean-ridge basalt [MORB], Saunders et al., Chap. 8, this volume) than the surrounding flows, and it would similarly have been intruded at a later stage in the development of the rift.

Lesher et al. (Chap. 12, this volume) interpret the oceanic flow of Unit 989-1 as erupted from a local center at the inner edge of the continent and not in the rift zone 30 km away. This also requires lateral injection of oceanic magma into the continental crust.

Oceanic basalts on a continental margin are rare but are also known from the Faeroe Islands. Here, Gariépy et al. (1983) and Hald and Waagstein (1991) described low-Ti basalts with oceanic chemistries very similar to that of the oceanic basalts described here. They form lava flows and are intruded as dikes within the lava plateau. The rift zone along the continent split runs west–east ~50 km north of the Faeroes (Smythe, 1983), and some of the dikes run west–east for 10–20 km and dip to the north (Hald and Waagstein, 1991). They probably fed lava flows. A similar situation can be envisaged for the Southeast Greenland margin.

Magma Fractionation and Formation of the Oceanic Crust

The oceanic lava flows have MgO = 8.23%–6.27% (volatile free) and do not represent primary magmas, which would have had much higher MgO contents. Thy et al. (1998, based on experiments) and Fitton et al. (1998b, based on fine-grained aphyric high-MgO rocks) estimated that the primary magmas for the Site 917 upper series contained up to 18% MgO. Demant (1998) found olivine with up to $Fo_{92.5}$ in a picrite from the Site 917 upper series, and, if this is a true phenocryst, it similarly indicates a very magnesian magma. Assuming that the mantle temperature stayed constant from the melting of the primary magmas of the Site 917 upper series to those of the primary magmas of Site 990/915, the removal of the continental lid and the resulting continued melting to shallower levels at Site 990/915 must have led to larger degrees of melting than for Site 917 (Fram et al., 1998). We thus estimate that the primary magma for the oceanic basalts also had around 18% MgO, and we put 20% MgO as a possible upper limit (the melt will then be in equilibrium with olivine $Fo_{92.0}$ at the fayalite-magnetite-quartz [FMQ] oxygen buffer). We have calculated possible primary magmas by adding equilibrium olivine to the most magnesian of the oceanic basalts (Unit 990–7) in 0.5% increments, assuming an iron-magnesium distribution coefficient between olivine and melt of 0.30 (Roeder and Emslie, 1970) and all iron as FeO. Unit 990-7 is slightly crustally contaminated (Ba/Zr = 0.53, the next lowest in the Site 990 lavas), but its SiO_2 is among the lowest found and was used without any correction. The calculated primitive magma with 18% MgO is shown in Table 2.

Fractionation calculations were then carried out on the primitive magma compositions with the computer program COMAGMAT (Ariskin et al., 1993), assuming water-free compositions at the FMQ oxygen buffer. This program utilizes a free energy minimization algorithm to calculate mineral-melt equilibria and crystallization temperature at a given pressure and percent crystallized. It is based on experiments conducted at 1 atm pressure but is calibrated at pressures up to 10–12 kbar, and temperatures are reproduced to within 15°–20°C (Ariskin et al., 1993). Calculations were carried out at a number of different pressures to study the effect of pressure on the results. The first part of the liquid line of descent is not pressure sensitive, but the later parts are. At all pressures, olivine first fractionates alone in amounts depending on the starting composition. At pressures ≥4 kbar, olivine is then joined or replaced by clinopyroxene. Considering the high Sc contents in the oceanic basalts (Fig. 6) and the high $D_{sc}^{cpx\text{-}liq}$ (0.51: Ulmer, 1989; up to 2.15: Rocholl et al., 1996), the amount of fractionating clinopyroxene is strongly limited, and pressures <4 kbar are more realistic for the later parts of the liquid line of descent. At 3 kbar, olivine is joined on the liquidus simultaneously by

plagioclase and clinopyroxene, giving rise to gabbro fractionation. Irrespective of the MgO content of the starting composition, this happens when the liquid has ~8.0% MgO (justifying the addition of olivine only to Unit 990-7 with 8.23% MgO in the calculation of the primary liquid). A pressure of 3 kbar corresponds to a depth of ~10 km and is a realistic estimate for the depth of the magma chambers in which the gabbro fractionation took place (Fig. 8). The preceding olivine fractionation would have taken place at similar and deeper levels, representing deep parts of the magma chambers and underlying magma conduits. Fram et al. (1998) modeled a pressure of 10 kbar for the top of the oceanic melting column, and this is thus a maximum pressure for the start of crystallization. The calculated proportions of fractionated phases are, however, insensitive to the starting pressure.

Table 2 shows the results of the COMAGMAT fractionation and temperature calculations starting from the primitive melt with 18% MgO (Table 2, column 1). Crystallization is started at a pressure of 7 kbar where the melt has a temperature of 1449°C, corresponding to a potential temperature of ~1400°C. The melt fractionates olivine during a pressure decrease (ascent of the melt) from 7 kbar to 3 kbar. After crystallization of 30 mol% olivine ($Fo_{91.2–82.1}$) the melt has ~8.0% MgO and a temperature of ~1200°C (Table 2, column 2). The calculated melt composition closely matches the measured composition of Unit 990–7 (Table 2, column 3). This is not coincidental since first adding equilibrium olivine to a composition and then removing it again (albeit with two different methods, a spreadsheet and a computer program) is bound to produce a match. The melt then crystallizes olivine, plagioclase, and clinopyroxene simultaneously in near-constant proportions, and an amount of 24% of this gabbro fractionation (Table 2, column 4) is required to reproduce the most evolved basalt, Unit 990-1 (Table 2, column 5). The modal composition (in vol%) of the gabbro cumulate is 8% olivine ($Fo_{81.9–73.6}$), 50% plagioclase ($An_{75.8–65.9}$), and 42% clinopyroxene ($Fs_{9.3–14.7}$).

The erupted oceanic magmas, with 8.23%–6.27% MgO, correspond very closely to those associated with the gabbro fractionation stage. It appears that the magmas had to fractionate almost to the point of three-phase cotectic relations before they were able to erupt. The average MgO content of the oceanic rocks from Sites 989, 990, 915, and 918 is 7.3%, corresponding to an average amount of gabbro fractionation of 14% of the primitive magma.

In conclusion, the COMAGMAT calculations show that the primitive magma with 18% MgO will fractionate into 30 mol% olivine cumulates, 14 mol% gabbro cumulates, and 56 mol% melt, which is intruded as dikes and erupted as lavas. If the magma is more magnesian, the proportion of olivine cumulates will increase (to 35 mol% for a melt with 20% MgO). The balance between the calculated amounts of gabbro cumulates and melt is strongly dependent on the average MgO content of the analyzed samples, but, on the other hand, the average of 7.3% ± 0.5% MgO (1σ) is fairly robust. The mode of the gabbro cumulates is also robust. What the calculations do not show, however, is the significant amount of melt that must be retained within the cumulates.

The results from the COMAGMAT calculations can be compared with the modeled crustal structure of H.C. Larsen et al. (1998), which is based on geophysical data and shown here in Figure 8. Outside the continental edge, the igneous part of the oceanic crust is constantly ~18 km thick (at 3–21-km depth) and consists of three units (3, 5, and 6 in Figure 8). H.C. Larsen et al. (1998) interpreted units 5 (4 km) and 6 (4.3 km) as respectively lighter and heavier plutonic residues and noted that the boundary between them is uncertain. Unit 3 (9.7 km) was interpreted as SDRS lava flows underlain by a zone of dikes. A depth of 9.7 km to the cumulates corresponds to a pressure of ~3 kbar, the pressure used in our calculations of the gabbro fractionation scheme.

Given a total igneous thickness of 18 km, our fractionation calculations set out above and in Table 2 translate into thicknesses of 5.4 km of olivine cumulates, 2.5 km of gabbro cumulates, and 10.1 km of dikes and lava flows, as set out in Table 3. The cumulate olivine ($Fo_{91–82}$) has a density around 3.35, and a gabbro with mineral mode and composition as given above will have an average density of 3.03 (olivine, 3.45; plagioclase, 2.72; clinopyroxene, 3.33). Any amount of melt retained in the cumulates will increase the thickness and decrease the densities of the cumulates and decrease the thickness of the layer of dikes and lava flows. While the total amount of calculated cumulates corresponds to that in the geophysical model, the proportions of light and heavy cumulates are different. However, velocity information from more recent crustal wide-angle seismic data along the same profile indicate that the amount of heavy cumulates in Figure 8 is significantly underestimated, while the amount of light cumulates is correspondingly overestimated. The thickness of the layer with dikes and lava flows is unchanged (T. Dahl-Jensen, pers. comm., 1997). The new data bring the geophysical model and the chemical composition derived model into broad agreement. The chemical data presented here thus support the modeling based on geophysical data and give an independent indication of the nature of the various layers in the oceanic crust.

Table 3. Thicknesses of the oceanic crustal layers in the Southeast Greenland SDRS.

	Calculated from basalt compositions			Geophysical model*	
	Mol%	Km	Density‡	Km	Density
Total igneous crust:	100	18.0†		18.0	
Olivine cumulates:	30	5.4	3.35	4.3	3.12
Gabbro cumulates:	14**	2.5	3.03	4.0	2.90
Dikes and lava flows:	56	10.1		9.7	2.80

Notes: * = Model from H.C. Larsen et al. (1998), based on reflection seismic and gravity data. † = Total melt km taken from geophysical model of H.C. Larsen et al. (1998). ** = Amount of gabbro cumulates calculated from average degree of fractionation of lavas in SDRS. ‡ = The calculated densities do not take any interstitial melt into account. See text for details.

CONCLUSIONS

1. The basaltic clasts in the cobble conglomerate that overlay the SDRS at Site 990 are probably derived from the Precambrian basement. They are unlikely to be derived from the Site 917 lower series, and there are, therefore, no positive indications that this series was exposed and being eroded at an early stage. The reason why the lower series is missing at Site 989 may rather be the depositional offlap of the volcanic pile toward the embryonic spreading center, although erosion or faulting cannot be excluded.

2. The lava flows drilled at Sites 989 and 990 all have chemical compositions similar to the previously drilled MORB-like (oceanic) postbreakup basalts of Sites 915 and 918. A dikelet from Site 990 and a previously drilled dike from Site 917 are similarly oceanic. We believe that the flows from Site 989 were emplaced after breakup despite their setting on the inner part of the continental margin.

3. The lava succession at Site 990 shows a slight development upsection, from less to more fractionated compositions (Mg# 62.3–49). However, the variation is within that displayed by the oceanic rocks as a whole, and the establishment of magma chambers in the newformed oceanic crust, characterizing the transition from the variable synbreakup conditions seen in the Site 917 upper series and to the uniform postbreakup conditions seen at Site 990, must be achieved during the deposition of the short undrilled lava succession between the two sites. The transition was accompanied by a decrease of about 3–5 kbar in the mean pressure of melting.

4. All the lava flows from Site 990 and one from Site 989 are contaminated with continental crustal material. Only flow Unit 989-1

and two dikes appear to be uncontaminated. The contamination probably took place in the magma chambers within the young oceanic rift when this still contained fragments of continental material. The lavas would be erupted within the rift and flow subaerially away from it and onto the continent. We predict that the contamination signal will rapidly decrease in the lava succession overlying that at Site 990.

5. The dikes show that lateral injection of oceanic magma into the continental crust also took place, even without ensuing contamination. The flows at Site 989 could have been erupted from such a dike. They constitute a rare example of oceanic basalts deposited on a continent.

6. The primitive magma that gave rise to the oceanic basalts had an estimated 18% MgO. After fractionation of 30 mol% olivine, it shifted to gabbro fractionation (olivine + plagioclase + clinopyroxene), and the melts started to erupt. The chemical variation within the erupted lavas (8.23%–6.27% MgO) can be explained by up to 24 mol% gabbro fractionation at 3 kbar (31%–54% in the fractionation scheme for the primitive magma), but the average amount of gabbro fractionation is only 14 mol% (giving the average MgO content of 7.3%). The figures 100% primitive melt = 30% olivine cumulates + 14% gabbro cumulates + 56% melts (dikes and lava flows) compare well with the thicknesses for the three igneous layers of the thick oceanic crust modeled from published and new geophysical data over the area and give an independent indication of the character of the layers in the oceanic crust.

ACKNOWLEDGMENTS

Henriette Hansen is thanked for introducing LML to the COMAGMAT program, and Trine Dahl-Jensen is thanked for discussions and permission to cite unpublished data. C.E. Lesher, J. Ludden, and J.A. Pearce provided constructive reviews. LML publishes with the permission of the Geological Survey of Denmark and Greenland.

REFERENCES

Ariskin, A.A., Frenkel, M.Y., Barmina, G.S., and Nielsen, R., 1993. COMAGMAT: A FORTRAN program to model magma differentiation processes. *Comput. Geosci.*, 19:1155–1170.

Demant, A., 1998. Mineral chemistry of volcanic sequences from Hole 917A, southeast Greenland margin. *In* Saunders, A.D., Larsen, H.C., and Clift, P. (Eds.), *Proc. ODP, Sci. Results.*, 152: College Station, TX (Ocean Drilling Program) 403–416.

Duncan, R.A., Larsen, H.C., Allan, J.F., et al., 1996. *Proc. ODP, Init. Repts*., 163: College Station, TX (Ocean Drilling Program).

Fitton, J.G., Saunders, A.D., Larsen, L.M., Fram, M.S., Demant, A., Sinton, C., and Leg 152 Shipboard Scientific Party, 1995. Magma sources and plumbing systems during break-up of the Southeast Greenland margin: preliminary results from ODP Leg 152. *J. Geol. Soc. London*, 152:985–990.

Fitton, J.G., Hardarson, B.S., Ellam, R.M., and Rogers, G., 1998a. Sr-, Nd-, and Pb-isotopic composition of volcanic rocks from the southeast Greenland Margin at 63°N: temporal variation in crustal contamination during continental breakup. *In* Saunders, A.D., Larsen, H.C., and Wise, S.H., Jr. (Eds.), *Proc. ODP, Sci. Results.*, 152: College Station, TX (Ocean Drilling Program), 351–357.

Fitton, J.G., Saunders, A.D., Larsen, L.M., Hardarson, B.S., and Norry, M.J., 1998b. Volcanic rocks from the southeast Greenland margin at 63°N: composition, petrogenesis, and mantle sources. *In* Saunders, A.D., Larsen, H.C., and Wise, S.H., Jr. (Eds.), *Proc. ODP, Sci. Results.*, 152: College Station, TX (Ocean Drilling Program), 331–350.

Fram, M.S., Lesher, C.E., and Volpe, A.M., 1998. Mantle melting systematics from continental to oceanic volcanism on the southeast Greenland Margin. *In* Saunders, A.D., Larsen, H.C., and Wise, S.H., Jr. (Eds.), *Proc. ODP, Sci. Results.*, 152: College Station, TX (Ocean Drilling Program), 373–386.

Gariépy, C., Ludden, J., and Brooks, C., 1983. Isotopic and trace element constraints on the genesis of the Faeroe lava pile. *Earth Planet. Sci. Lett.*, 63:257–272.

Hald, N., and Waagstein, R., 1991. The dikes and sills of the Early Tertiary Faeroe Island basalt plateau. *Trans. R. Soc. Edinburgh: Earth Sci*., 82:373–388.

Heinrich, K.F.J., 1966. X-ray absorption uncertainty. *In* McKinley, T.D., Heinrich, K.F.J., and Wittry, D.B. (Eds.), *The Electron Microprobe*: New York (John Wiley and Sons), 296–377.

Kinzler, R.J., and Grove, T.L., 1992. Primary magmas of mid-ocean ridge basalts, 2. Applications. *J. Geophys. Res.*, 97:6907–6926.

Kinzler, R.J., and Grove, T.L., 1993. Corrections and further discussion of the primary magmas of mid-ocean ridge basalts, 1 and 2. *J. Geophys. Res.*, 98:22339–22347.

Langmuir, C.H., Klein, E., and Plank, T., 1992. Petrological systematics of mid-ocean ridge basalts: constraints on melt generation beneath ocean ridges. *In* Morgan, J., Blackman, D., Sinton, J. (Eds.), *Mantle Flow and Melt Generation at Mid-Ocean Ridges.* Geophys. Monogr., Am. Geophys. Union, 71:183–280.

Larsen, H.C., and Saunders, A.D., 1998. Tectonism and volcanism at the Southeast Greenland rifted margin: a record of plume impact and later continental rupture. *In* Saunders, A.D., Larsen, H.C., and Wise, S.H., Jr. (Eds.), *Proc. ODP, Sci. Results*., 152: College Station, TX (Ocean Drilling Program), 503–533.

Larsen, H.C., Saunders, A.D., Clift, P.D., et al., 1994. *Proc. ODP, Init. Repts.*, 152: College Station, TX (Ocean Drilling Program).

Larsen, H.C., Dahl-Jensen, T., and Hopper, J.R., 1998. Crustal structure along the Leg 152 drilling transect. *In* Saunders, A.D., Larsen, H.C., and Wise, S.H., Jr. (Eds.), *Proc. ODP, Sci. Results*., 152: College Station, TX (Ocean Drilling Program), 463–475.

Larsen, L.M., Fitton, J.G., and Fram, M.S., 1998a: Volcanic rocks of the southeast Greenland Margin in comparison with other parts of the North Atlantic tertiary igneous province. *In* Saunders, A.D., Larsen, H.C., and Wise, S.H., Jr. (Eds.), *Proc. ODP, Sci. Results*., 152: College Station, TX (Ocean Drilling Program), 315–330.

Larsen, L.M., Fitton, J.G., Bailey, J.C., and Kystol, J., 1998b: XRF analyses of volcanic rocks from Leg 152 by laboratories in Edinburgh and Copenhagen: implications for the mobility of yttrium and other elements during alteration. *In* Saunders, A.D., Larsen, H.C., and Wise, S.H., Jr. (Eds.), *Proc. ODP, Sci. Results.*, 152: College Station, TX (Ocean Drilling Program), 425–429.

McKenzie, D., and Bickle, M.J., 1988. The volume and composition of melt generated by extension of the lithosphere. *J. Petrol.*, 29:625–679.

Niu, Y., and Batiza, R., 1991. An empirical method for calculating melt compositions produced beneath mid-ocean ridges: application for axis and off-axis (seamount) melting. *J. Geophys. Res.*, 96:21753–21777.

Rocholl, A., Ludwig, T., Altherr, R., Meyer, H.-P., Brey, G., Velz, S., Seck, H.-A., and Bulatov, V., 1996. Experimental partitioning of trace elements between clinopyroxene, garnet and basanitic melts studied by ion microprobe. *J. Conf. Abstr.*, 1:517–518.

Roeder, P.L., and Emslie, R.F., 1970. Olivine-liquid equilibrium. *Contrib. Mineral. Petrol.*, 29:275–289.

Saunders, A.D., Fitton, J.G., Kerr, A.C., Norry, M.J., and Kent, R.W., 1997. The North Atlantic igneous province. *In* Mahoney, J.J., and Coffin, M.F. (Eds.), *Large Igneous Provinces.* Am. Geophys. Union., Geophys. Monogr., 100:45–93.

Saunders, A.D., Larsen, H.C., and Fitton, J.G., 1998. Magmatic development of the southeast Greenland Margin and evolution of the Iceland plume: geochemical constraints from Leg 152. *In* Saunders, A.D., Larsen, H.C., and Wise, S.H., Jr. (Eds.), *Proc. ODP, Sci. Results*., 152: College Station, TX (Ocean Drilling Program), 479–501.

Sinton, C.W., and Duncan, R.A., 1998. ^{40}Ar-^{39}Ar ages of lavas from the southeast Greenland Margin, ODP Leg 152 and the Rockall Plateau, DSDP Leg 81. *In* Saunders, A.D., Larsen, H.C., Clift, P.D., and Wise, S.W., Jr. (Eds.), *Proc. ODP, Sci. Results*, 152: College Station, TX (Ocean Drilling Program), 387–402.

Smythe, D.K., 1983. Faeroe-Shetland escarpment and continental margin north of the Faeroes. *In* Bott, M.H.P., Saxov, S., Talwani, M., and Thiede,

J. (Eds.), *Structure and Development of the Greenland-Scotland Ridge.* New York (Plenum), 109–119.

Thy, P., Lesher, C.E., and Fram, M.S., 1998. Low pressure experimental constraints on the evolution of basaltic lavas from Site 917, southeast Greenland continental margin. *In* Saunders, A.D., Larsen, H.C., Clift, P.D., and Wise, S.W., Jr. (Eds.), *Proc. ODP, Sci. Results*, 152: College Station, TX (Ocean Drilling Program), 359–372.

Ulmer, P., 1989. Partitioning of high-field strength elements among olivine, pyroxenes, garnet and calc-alkaline picrobasalt; experimental results and an application. *Ann. Rep., Director Geophys. Lab., Carnegie Inst. Washington, 1988–1989*, 42–47.

Waagstein, R., 1988. Structure, composition and age of the Faeroe basalt plateau. *In* Morton, A.C., and Parson, L.M. (Eds.), *Early Tertiary Volcanism and the Opening of the NE Atlantic.* Geol. Soc. Spec. Publ. London, 39:225–238.

Wilson, A.D., 1955. A new method for the determination of ferrous iron in rocks and minerals. *Bull. Geol. Surv. G.B.*, 9:56–58.

Date of initial receipt: 14 January 1998
Date of acceptance: 5 June 1998
Ms 163SR-109